Notch1 modulates timing of G_1-S progression by inducing SKP2 transcription and $p27^{Kip1}$ degradation

Leonor M. Sarmento,[1,4] Hui Huang,[1] Ana Limon,[1,5] William Gordon,[1] Jacquenilson Fernandes,[1] Maria J. Tavares,[3] Lucio Miele,[6] Angelo A. Cardoso,[3] Marie Classon,[2] and Nadia Carlesso[1]

[1]Center of Regenerative Medicine and Technology, [2]Cancer Center, Massachusetts General Hospital, and [3]Department of Medical Oncology, Dana-Farber Cancer Institute, Harvard Medical School, Boston, MA 02129
[4]IMM, Institute of Molecular Medicine, University of Lisbon, 1649-028 Lisbon, Portugal
[5]Science Research Laboratory Inc., Somerville, MA 02143
[6]Department of Pharmacodynamics, University of Illinois, Chicago, IL 60612

Cyclin-dependent kinase inhibitors (CKIs) and Notch receptor activation have been shown to influence adult stem cells and progenitors by altering stem cell self-renewal and proliferation. Yet, no interaction between these molecular pathways has been defined. Here we show that ligand-independent and ligand-dependent activation of Notch1 induces transcription of the S phase kinase–associated protein 2 (SKP2), the F-box subunit of the ubiquitin-ligase complex SCF^{SKP2} that targets proteins for degradation. Up-regulation of SKP2 by Notch signaling enhances proteasome-mediated degradation of the CKIs, $p27^{Kip1}$ and $p21^{Cip1}$, and causes premature entry into S phase. Silencing of SKP2 by RNA interference in G_1 stabilizes $p27^{Kip1}$ and $p21^{Cip1}$ and abolishes Notch effect on G_1-S progression. Thus, SKP2 serves to link Notch1 activation with the cell cycle machinery. This novel pathway involving Notch/SKP2/CKIs connects a cell surface receptor with proximate mediators of cell cycle activity, and suggests a mechanism by which a known physiologic mediator of cell fate determination interfaces with cell cycle control.

CORRESPONDENCE
Nadia Carlesso:
carlesso.nadia@mgh.harvard.edu

Abbreviations used: ATRA, all-trans-retinoic acid; CDK, cyclin-dependent kinase; CKI, cyclin-dependent kinase inhibitor; ΔE, intracellular with transmembrane domain of Notch; Dll, Delta-like; EMSA, electrophoretic mobility shift assay; GSI, γ-secretase inhibitor; ICN, intracellular domain of Notch; IP, immunoprecipitation; J1, Jagged1; J2, Jagged2; N1, Notch1; N1AS, N1 antisense; $Notch^{ic}$, Notch intracellular domain; SCF, SKP1/CUL1/F-box; siRNA, small interfering RNA; SKP2, S phase kinase–associated protein 2.

Members of the Notch/Lin12 family are highly conserved transmembrane receptors that influence the cell fate of diverse types of precursor cells in a variety of multicellular organisms (1). Physiologic activation of Notch signaling requires cell–cell contact and occurs through binding of the Notch receptor to one of its ligands (Delta, Serrate/Jagged), followed by proteolytic release of the Notch intracellular domain ($Notch^{ic}$) and its translocation to the nucleus (2). $Notch^{ic}$ interacts with CSL transcription factors (CBF1, Su(H), Lag-1) and converts them from repressors to activators, promoting transcription of downstream genes involved in various differentiation programs (3).

In many cellular systems, Notch activation affects the finely tuned balance between proliferation and differentiation that regulates the stem and progenitor cell pools (1, 4, 5). Regulation of cell differentiation and cell fate decision by Notch is achieved by induction of specific differentiation programs and by an independent regulation of the cell cycle. Notch activation has been shown to induce alterations of the cell cycle kinetics that precede the inhibition of myeloid differentiation in hematopoietic cells (6), and to influence keratinocyte differentiation by two distinct mechanisms that involve induction of cell cycle arrest through $p21^{Cip1}$ and transcriptional regulation of specific genes (4).

Regulation of the cell cycle by Notch signaling involves the coordination of different, and sometimes antagonizing, pathways in a highly cell context–dependent manner. For example, Notch activation has been found to induce proliferation of kidney epithelial cells through induction of cyclin D_1 (7), and to lead to cell cycle arrest in keratinocytes through induction of $p21^{Cip1}$ (4). These observations indicate the existence of multiple alternative molecular interactions between Notch signaling and the cell cycle machinery, which are

The online version of this article contains supplemental material.

JEM © The Rockefeller University Press $8.00
Vol. 202, No. 1, July 4, 2005 157–168 www.jem.org/cgi/doi/10.1084/jem.20050559

likely to correlate with the ability of Notch to function as an oncogene or a tumor suppressor (8, 9).

Physiologic regulation of the G_1-S transition is critical during determination of cell fate and is lost during oncogenic transformation. Cyclin-dependent kinases (CDKs) and cyclin-dependent kinase inhibitors (CKIs) play key roles in regulating cell cycle progression from G_1 to S phase (10). Absence of the CKIs, $p21^{Cip1}$ or $p27^{Kip1}$, affect self-renewal of hematopoietic stem cells (11) and the proliferation/differentiation balance of hematopoietic progenitors (12), respectively, and predispose cells to neoplastic transformation (13).

In this study, we explore the role of Notch signaling at the defined G_1–S phase transition of the cell cycle. We found that Notch1 (N1) activation reduces the permanence of the cells in G_1 and accelerates their entry into S phase by promoting transcriptional induction of the F-box protein, SKP2, and in turn, proteasome-mediated degradation of the CKIs, $p21^{Cip1}$ and $p27^{Kip1}$ (14, 15). Thus, enhancement of SKP2 transcription represents a mechanism by which Notch modulates timing of cell cycle progression and coordinates proliferation and differentiation decisions.

RESULTS

Notch1 activation induces premature cell cycle entry and its effect is enhanced by the lack of $p21^{Cip1}$

We demonstrated previously that N1 activation induces a more rapid G_1-S transition in hematopoietic progenitors (6). To identify the mechanisms that mediate this effect, we determined whether the alterations in cell cycle kinetics caused by N1 activation were enhanced in the absence of the G_1 regulatory molecule, $p21^{Cip1}$, which was shown to mediate Notch-induced cell cycle arrest in some cell types (4). WT and $p21^{Cip1}$ knock-out ($p21^{-/-}$) 3T3 fibroblasts transduced with the retroviral bicistronic construct MSCV-GFP containing the constitutively activated forms of N1, (ICN) intracellular domain of Notch, and ΔE (intracellular with transmembrane domain of Notch) (Fig. S1, available at http://www.jem.org/cgi/content/full/jem.20050559/DC1) were synchronized by nocodazole block-and-release and screened for alterations in the G_1 to S phase transition. This analysis (Fig. 1, A and B) showed that constitutively active N1 increases the percentage of cells in S phase in WT cells (+10–15%) and that the magnitude of this effect is significantly greater in the absence of $p21^{Cip1}$ (+20–30%). Despite the effects of N1 on cell cycle kinetics, Notch activation did not affect the overall cell cycle length and cell proliferation (Fig. 1 C). Preservation of total cell cycle length has been also observed in other 3T3 cells in which the G_1 phase of the cell cycle was shortened (16). Furthermore, overexpression of constitutively active N1 did not induce transformation in WT or $p21^{-/-}$ fibroblasts, as measured by soft agar colony assays (unpublished data).

These results show that the expression of constitutively active N1 in 3T3 fibroblasts accelerates G_1 transition without increasing rates of proliferation, and that this effect is enhanced by the lack of the CKI, $p21^{Cip1}$. Furthermore, these observations suggest that additional cell cycle regulators mediate Notch effects on the cell cycle and that $p21^{Cip1}$ may play a role in balancing such effects.

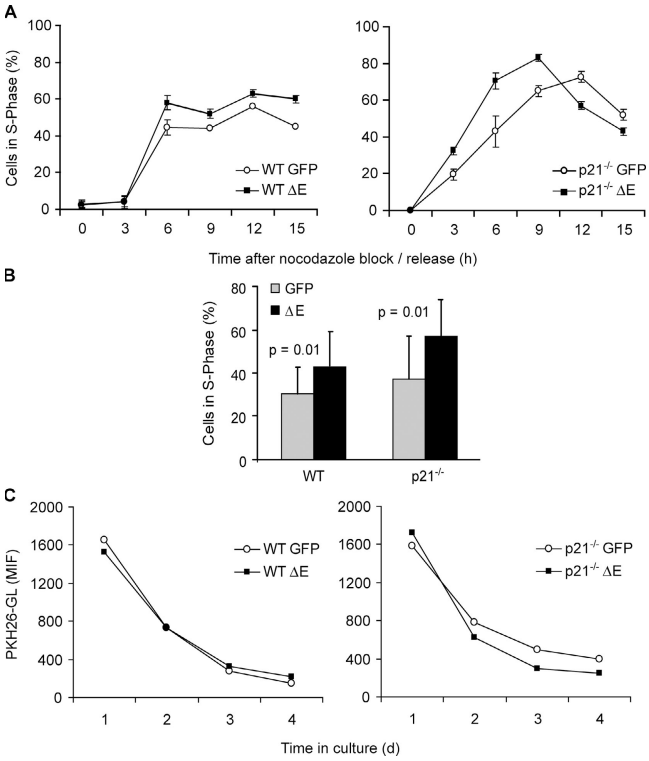

Figure 1. Biologic effects of N1 activation on 3T3 WT and $p21^{-/-}$ fibroblasts. (A) Percentage of cells in S phase during cell cycle progression. The cell cycle entry of transduced 3T3 cells was evaluated by bromodeoxyuridine incorporation. Values represent an average of duplicate samples in a representative experiment. (B) Bars indicate the average percentage of cells in S phase at 6 h after nocodazole block and release in five independent experiments. The difference between GFP and ΔE populations is statistically significant. (C) Cell division kinetics. Cells stained with PKH26-GL were seeded at low density and analyzed by FACS. The line graphs show a representative experiment. Values indicate PKH 26-GL mean intensity of fluorescence (MIF), decaying over time during cells' exponential growth.

Notch1 activation induces $p27^{Kip1}$ down-regulation and enhances CDK2 kinase activity

Next, we determined whether N1 activation altered the activity of CDK2 or CDK4 complexes, both critical for S phase entry and progression. WT and $p21^{-/-}$ 3T3 cells transduced with constitutively active N1 exhibited a significant increase in CDK2 kinase activity compared with control cells, whereas no significant differences were observed in CDK4 activity (Fig. 2 A). The greater kinase activity was not due to increased cyclin levels because all cell lines expressed similar levels of cyclin D_1, A, and E, as well as CDK2 and CDK4 (Fig. 2 B).

Because CDK2 activity is antagonized strongly by the CKIs of the Cip/Kip family, $p21^{Cip1}$ and $p27^{Kip1}$, we tested

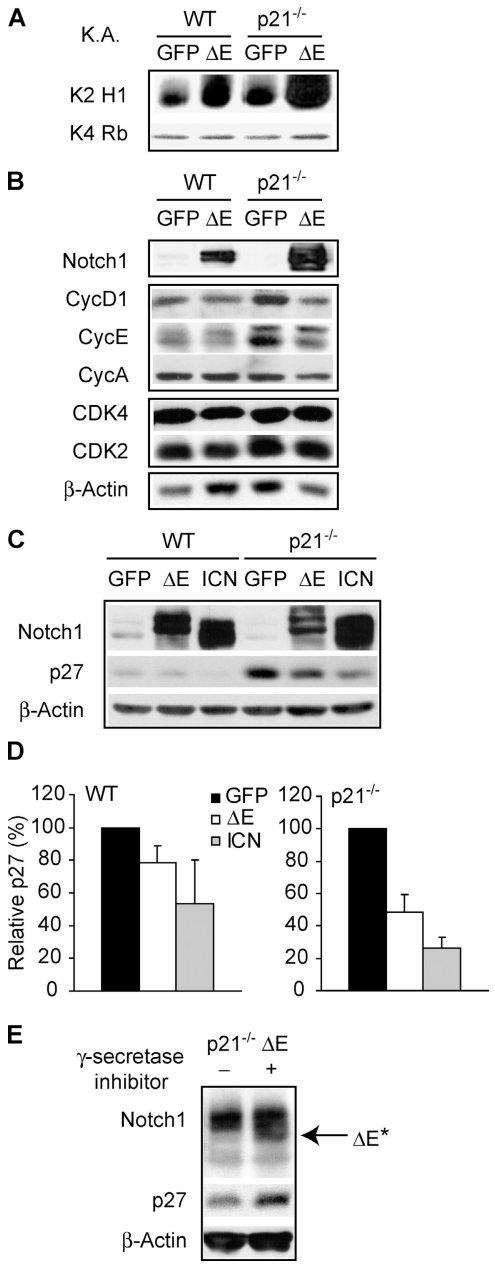

Figure 2. N1 activation correlates with increased CDK2 kinase activity and promotes $p27^{Kip1}$ down-regulation. (A) In vitro kinase activity assay (K.A.) of immunoprecipitated CDK2 (K2) or CDK4 (K4) complexes from growing cells. Histone (H1) or retinoblastoma (Rb) was used as substrate, respectively. (B) Immunoblot of cyclins and CDKs. (C) Immunoblot of $p27^{Kip1}$. $p21^{-/-}$ cells express higher levels of $p27^{Kip1}$ compared with WT, perhaps as a compensatory mechanism. In this blot, where WT and $p21^{-/-}$ cells are side by side, $p27^{Kip1}$ in WT samples is underexposed to avoid its overexposure in $p21^{-/-}$ samples. (D) ImageQuant densitometric analysis of $p27^{Kip1}$ protein expression. The values, an average of five independent experiments, indicate percentage of $p27^{Kip1}$ protein detected in ΔE or ICN cells relative to their GFP controls (100%). (E) Cells were incubated with the GSI (+) or DMSO vehicle control (−) for 12 h. Protein extracts from harvested cells were analyzed by Western blot to assess N1 and $p27^{Kip1}$ expression.

the possibility that the greater CDK2 kinase activity observed in the presence of N1 in WT and $p21^{-/-}$ cells was due to a lower level of CDK2 inhibition by decreased levels of $p27^{Kip1}$. We found that $p27^{Kip1}$ expression was significantly lower in WT and $p21^{-/-}$ cells transduced with constitutively active N1 (Fig. 2 C and Fig. 3 A). In the WT background, $p27^{Kip1}$ levels in ΔE and ICN cells were 80 and 60% of control GFP cells, respectively; in the $p21^{-/-}$ background, $p27^{Kip1}$ levels in ΔE and ICN cells were 50 and 30% of control GFP cells, respectively (Fig. 2 D).

To confirm that $p27^{Kip1}$ down-regulation was a direct consequence of Notch activity, 3T3 cells expressing constitutively active N1 were treated with a γ-secretase inhibitor (GSI). GSIs have been shown to impair activation of full-length Notch and Notch/ΔE by blocking the proteolytic intracytoplasmic cleavage that occurs in membrane-tethered forms of Notch (17). Inhibition of this process blocks the generation of the active cleaved form of Notch, $Notch^{ic}$, and results in the accumulation of an intermediate inactive form of Notch, the metalloprotease cleavage product (ΔE⋆; reference 18). Treatment of $p21^{-/-}$ΔE cells with GSI caused the inhibition of Notch cleavage and could be observed as an accumulation of ΔE⋆ polypeptide. Block of Notch signaling by GSI resulted in the abolishment of Notch-induced $p27^{Kip1}$ down-regulation (Fig. 2 E). Thus, activation of N1 induces a specific down-regulation of $p27^{Kip1}$ in asynchronous WT and $p21^{-/-}$ cells.

Notch1 activation promotes $p27^{Kip1}$ ubiquitin-mediated degradation

To explore the molecular bases for N1-induced $p27^{Kip1}$ down-regulation, we tested whether this effect was dependent on the proteasome-degradation pathway, which is the prevalent mechanism of $p27^{Kip1}$ regulation in many cellular systems (19). Treatment with the 26S proteasome-specific inhibitor, lactacystin, reestablished high levels of $p27^{Kip1}$ in WT and $p21^{-/-}$ cells overexpressing constitutively active N1 (ΔE and ICN; Fig. 3 A); this confirmed the involvement of this pathway in Notch-mediated $p27^{Kip1}$ down-regulation. We further investigated $p27^{Kip1}$ half-life by treating ICN-expressing cells and controls with 10 μM of the ribosomal complex inhibitor, cycloheximide. As shown in Fig. 3 B, $p27^{Kip1}$ disappears more rapidly in ICN cells than in controls, showing a shorter half-life of $p27^{Kip1}$ in the presence of activated N1 (<2 h in ICN cells versus 4 h in controls). Finally, to determine if N1 activation enhances $p27^{Kip1}$ ubiquitination, we evaluated $p27^{Kip1}$ ubiquitinated forms in vivo. Endogenous $p27^{Kip1}$ was immunoprecipitated from extracts of ΔE and control cells that had been treated with the proteasome inhibitor, MG132, which is used to stabilize ubiquitinated intermediates. MG132 treatment had the same effects as did lactacystin treatment on GFP and ΔE cells (Fig. S2, available at http://www.jem.org/cgi/content/full/jem.20050559/DC1). Immunoprecipitates were subjected to immunoblot analysis with anti-$p27^{Kip1}$ antibodies to de-

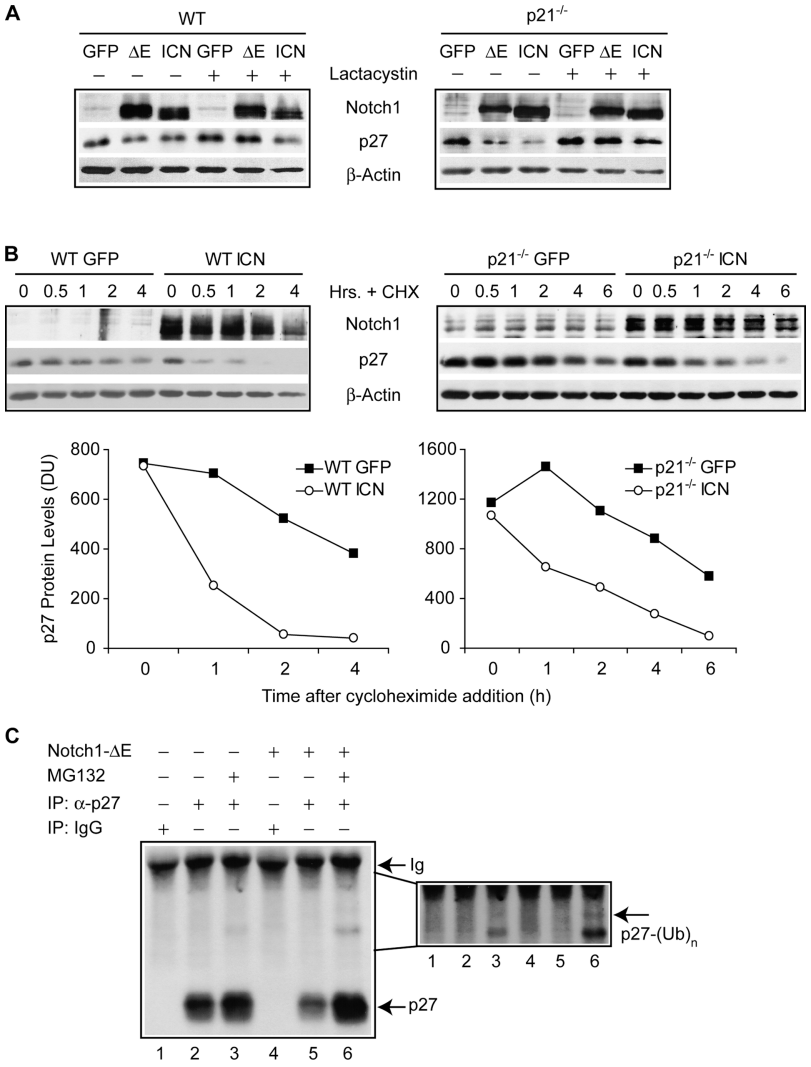

Figure 3. N1 activation induces ubiquitin–proteasome–mediated degradation of $p27^{Kip1}$. (A) Proteasome inhibition. Transduced 3T3 cells were incubated with DMSO (vehicle control) or the proteasome inhibitor, lactacystin. Cell extracts were analyzed by Western blot for $p27^{Kip1}$ expression. (B) $p27^{Kip1}$ protein half-life. Transduced 3T3 cells were arrested by nocodazole block. Cycloheximide was added 6 h after release into cell cycle and samples were incubated with cycloheximide for the indicated time points before lysis. $p27^{Kip1}$ protein levels were determined by Western blot (top panel) and their densitometric values normalized to β-actin, densitometric units (DU) were plotted as line graphs (bottom panel). (C) In vivo detection of ubiquitin conjugates. Cell extracts from $p21^{-/-}$ GFP and ΔE cells treated with MG132 or DMSO, were immunoprecipitated with anti-$p27^{Kip1}$ antibodies or with IgG controls, separated by SDS-PAGE and blotted with anti-$p27^{Kip1}$ antibodies. The inset shows a darker exposure of the blot for detection of slowly migrating forms of $p27^{Kip1}$.

tect the different migrating forms of $p27^{Kip1}$ (Fig. 3 C). Under these conditions, $p27^{Kip1}$ showed a basal level of ubiquitination that was increased significantly in the presence of N1 activation. Only $p27^{Kip1}$ immunoprecipitates from cells overexpressing ΔE treated with MG132 contained detectable levels of slow migrating polyubiquitinated derivatives (inset, Fig. 3 C, lanes 3 and 6). Presence of more highly ubiquitinated forms could not be detected due to interference with the assay by IgG heavy chain. Together, these findings show that N1 activation results in a rapid decrease of $p27^{Kip1}$ levels by enhancing proteasome-mediated degradation of the $p27^{Kip1}$ protein.

Notch1 regulates SKP2 and $p27^{Kip1}$ levels in a cell cycle–dependent manner

Because $p27^{Kip1}$ degradation is regulated by the SKP1/CUL1/F-box $(SCF)^{SKP2}$-ubiquitination complex during cell cycle progression (14), we tested the hypothesis that Notch activation decreased $p27^{Kip1}$ levels by regulating molecules that are involved in its degradation (e.g., the F-box protein, SKP2). We determined whether N1 activation altered the kinetics of SKP2 expression during cell cycle progression. In cells synchronized by nocodazole block-release or by serum starvation-stimulation, entry into the cell cycle was characterized by the induction of SKP2 pro-

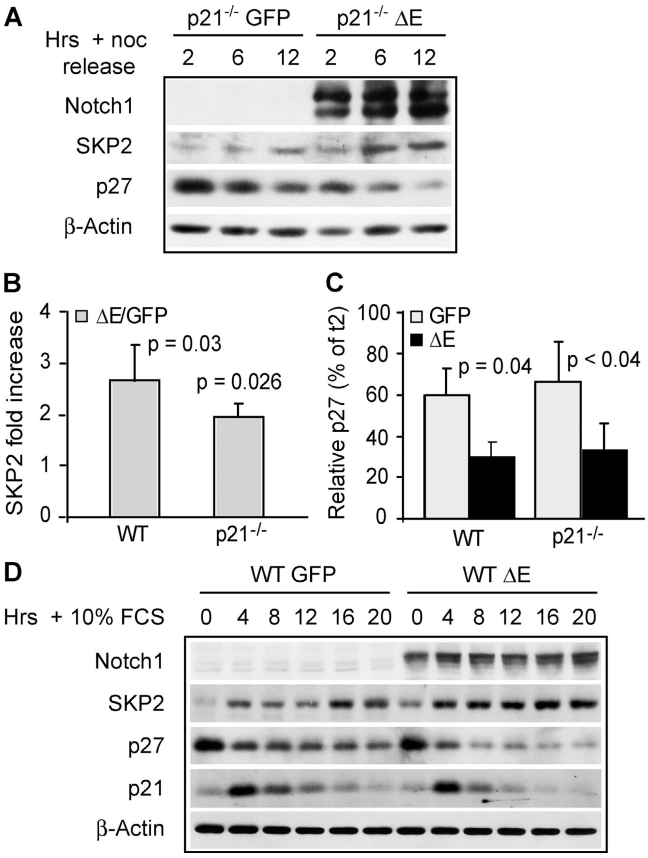

Figure 4. N1 activation enhances SKP2 expression and p27^{Kip1} degradation during cell cycle progression. (A) Immunoblot of SKP2 and p27^{Kip1} during cell cycle progression induced by nocodazole block and release. (B) SKP2 expression at 6 h from nocodazole block and release was quantified by densitometric analysis and normalized with β-actin expression in Western blots of three independent experiments. Bars express average fold increase of SKP2 expression in ΔE cells compared with GFP. (C) Bars represent average percentage of p27^{Kip1} expression at 6 h relative to 2 h (100%) in four independent experiments. (D) Immunoblot of SKP2, p21^{Cip1}, and p27^{Kip1} during serum-induced cell cycle progression.

tein in both GFP and ΔE cells. However, such induction was more rapid and greater in the presence of activated N1 than in control cells (Fig. 4, A and D). SKP2 levels were consistently two- to threefold higher in ΔE cells than in controls (Figs. 4 B and 5 B), and were especially higher at the early time points of cell cycle entry. The more rapid increase of SKP2 protein in ΔE cells was paralleled remarkably by a more rapid and significant degradation of p27^{Kip1} in these cells (Fig. 4, A, C, and D; and Fig. 5 B). At 6 h from nocodazole block release, p27^{Kip1} expression in ΔE cells decreased an average of 70% from the initial level, whereas it decreased only an average of 40% in control cells (Fig. 4 C). Recently, p21^{Cip1} was reported to be a target of the SCF^{SKP2} complex (15). Similar to p27^{Kip1}, p21^{Cip1} was down-regulated faster in ΔE-expressing cells than in control cells (Fig. 4 D; Fig. 5, A and B).

To demonstrate further the role of SKP2 in N1-mediated p27^{Kip1} degradation, GFP and ΔE cells were transfected with small interfering RNA (siRNA) against SKP2 during serum-induced cell cycle entry. Transfection of the siRNA against SKP2, but not a control siRNA, decreased the level of SKP2 to the limit of detection and prevented N1-induced p27^{Kip1} and p21^{Cip1} degradation (Fig. 5, A and B). Accumulation of p27^{Kip1}, consequent to SKP2 depletion, was equivalent in GFP and ΔE cells and resulted in an overall delay of cell cycle entry, as reported by previous studies (20, 21). Evaluation of S phase by Bromodeoxyuridine incorporation indicated that in the presence of equivalent levels of p27^{Kip1}, the effect of activated N1 on cell cycle entry was reduced dramatically (Fig. 5 C). In conclusion, these experiments show that N1 activation has a direct impact on the kinetics of SKP2 expression during cell cycle progression, and that this effect correlates with decreased levels of the CKIs, p27^{Kip1} and p21^{Cip1}. Furthermore, we demonstrated that SKP2 induction by N1 is required for Notch-induced down-regulation of p27^{Kip1} (and p21^{Cip1}) and consequent modulation of cell cycle progression.

Notch1 activation induces CBF-1–dependent transcription of SKP2

Because the SKP2 promoter is targeted for regulation during cell cycle progression and Notch promotes transcription of several target genes through activation of the CBF-1/RBP-Jκ transcription factor (4, 7), we hypothesized that Notch signaling may regulate SKP2 at a transcriptional level. We performed Northern blot quantification of SKP2 mRNA during cell cycle progression, and we found that SKP2 transcripts appear earlier and are more abundant in cells expressing activated N1 than in controls (Fig. 6, A and B).

To define better the mechanism of induction of SKP2 mRNA by Notch, we searched for possible regulatory elements in the human SKP2 promoter region. We identified and cloned a 3.1-kb region within the SKP2 promoter containing the sequence TGGGAA at position –350 that fully matches the consensus sequence of the high-affinity binding site for CBF-1/RBP-Jκ (22), schematically represented in Fig. 6 C. This consensus sequence is identical to the one present in the murine HES-1 and p21^{Cip1} promoters (Fig. 6 C), which is transactivated by the Notch^{ic}/CBF-1 complex (23). Electrophoretic mobility shift assay (EMSA) analysis showed that the protein-DNA complex could be identified only when the radiolabeled SKP2 WT oligonucleotide was incubated with extracts from 293T cells overexpressing CBF-1 (Fig. 6 D, lanes 2, 3, and 10); this confirmed the ability of CBF-1 to bind to the identified SKP2 sequence. The CBF-1–DNA complex was supershifted specifically by the anti–CBF-1 (lane 6 and 7) and by the anti-N1 (lane 9) antibodies, but not by an unrelated antibody (lane 10); its formation was abolished by excess of unlabeled WT but not mutated SKP2 oligonucleotide (lanes 4, 8 and 5). In the nucleus, N1 physically associates with CBF-1, promoting transcriptional activ-

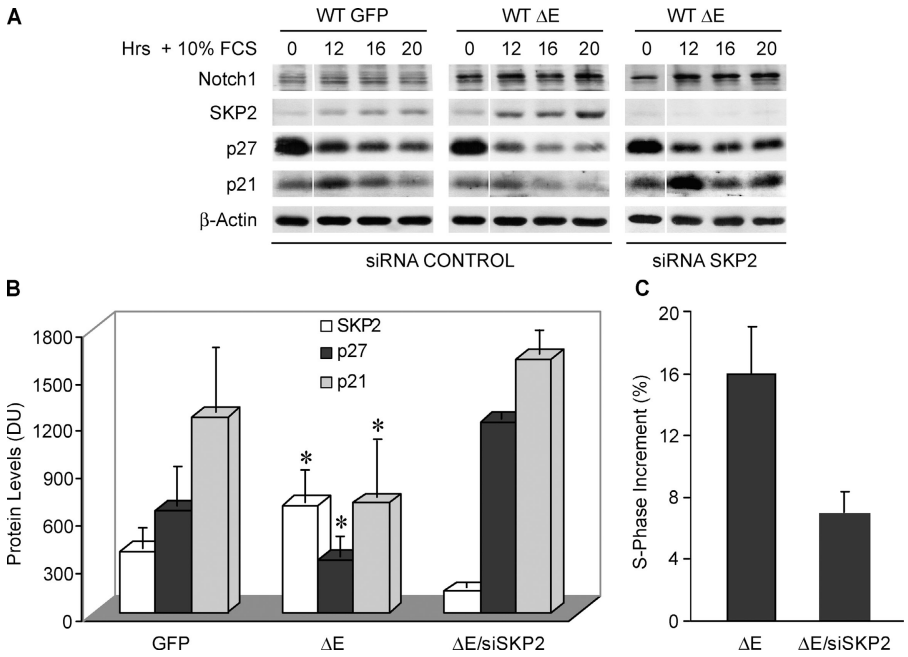

Figure 5. SKP2 is required for Notch effect on $p27^{Kip1}$. (A) WT-GFP and WT-ΔE were transfected with siRNA against SKP2 or GFP (negative control) during the serum starvation-stimulation procedure. Cell extracts were obtained at each indicated time point and analyzed by Western blot. The white lines indicate that intervening lanes have been spliced out. (B) Histogram summarizes multiple experiments at 12 h after serum stimulation. SKP2, $p27^{Kip1}$, and $p21^{Cip1}$ protein levels were quantified from Western blot bands and normalized with β-actin values. Bars represent average densitometric units of four independent observations for GFP and ΔE cells, and two independent observations for ΔE cells in the presence of siSKP2. (*) Statistically significant differences between ΔE and GFP cells: SKP2 $P = 0.015$; $p27^{Kip1}$ $P = 0.033$; $p21^{Cip1}$ $P < 0.003$. (C) Cells stimulated with serum in the absence or presence of SKP2 siRNA were pulsed with bromodeoxyuridine at 8 h and 12 h after stimulation. The difference between percentages of cells in S phase in ΔE and GFP cells were calculated. Bars represent averages of the differences expressed as percentage of S phase increment.

ity (23). To determine whether the Notch/CBF-1 complex binds to the endogenous SKP2 promoter, we performed chromatin immunoprecipitation assay with anti–CBF-1 or anti-N1 antibodies, followed by PCR amplification of the SKP2 promoter region. Only DNA coprecipitated with anti–CBF-1 or anti-N1 antibodies generated positive PCR products for the SKP2 promoter region containing the fully conserved CBF-1 binding site (Fig. 6 E). PCR of the Hes1 promoter region containing the CBF-1 site and of the CD11b promoter not containing the CBF-1 site, were performed as positive and negative controls, respectively.

To determine whether activated Notch induces CBF-1-dependent SKP2 transcription, we performed luciferase reporter assays on 3T3 fibroblasts following ΔE or ICN transduction. Constitutive activation of N1 correlated with significant transactivation of HES-1 and SKP2 promoters (Fig. 6 F). SKP2 promoter activity increased ~4- to 10-fold in cells overexpressing activated N1 (ΔE and ICN) compared with controls and paralleled HES-1 promoter activity, which was used as a positive control for CBF-1–dependent activity. Deletion of the CBF-1 binding motif resulted in the abrogation of transcriptional activation (Fig. 6 G). In conclusion, these data demonstrate that N1 activation promotes CBF-1–dependent transcription of SKP2.

SKP2 expression is induced in vivo by physiologic activation of endogenous Notch1 by its ligand

To confirm the physiologic relevance of our findings, we determined whether SKP2 expression could be induced by ligand-dependent stimulation of endogenous Notch in hematopoietic cells. These cells express Notch receptors and, in the BM microenvironment, are surrounded by neighboring cells expressing the Notch ligands Jagged1 (J1), Jagged2 (J2), Delta-like (Dll)1, and Dll4 (reference 24). We demonstrated previously that J2-dependent stimulation of the hematopoietic cells HL-60 results in accelerated G_1-S transition and in delayed myeloid differentiation in the presence of all-trans-retinoic acid (ATRA; reference 6). We generated murine stromal MS5 cell lines (25) overexpressing each of the Notch ligands (J1, J2, Dll1, and Dll4) and screened their effect on HL-60 cells. This analysis indicated that Dll4 induces the strongest inhibitory effect on HL60 cell differentiation, which is recapitulated by a recombinant Dll4-Fc fusion protein (unpublished data). Next, we determined whether Dll4-dependent stimulation of endogenous N1 induced SKP2 expression and $p27^{Kip1}$ down-regulation in HL-60 cells (Fig. 7 A). Incubation with Dll4 ligand induced strong activation of Notch signaling, confirmed by the induction of the cleaved active form of N1, $Notch^{ic}$ (Fig. 7 B). N1 activation upon

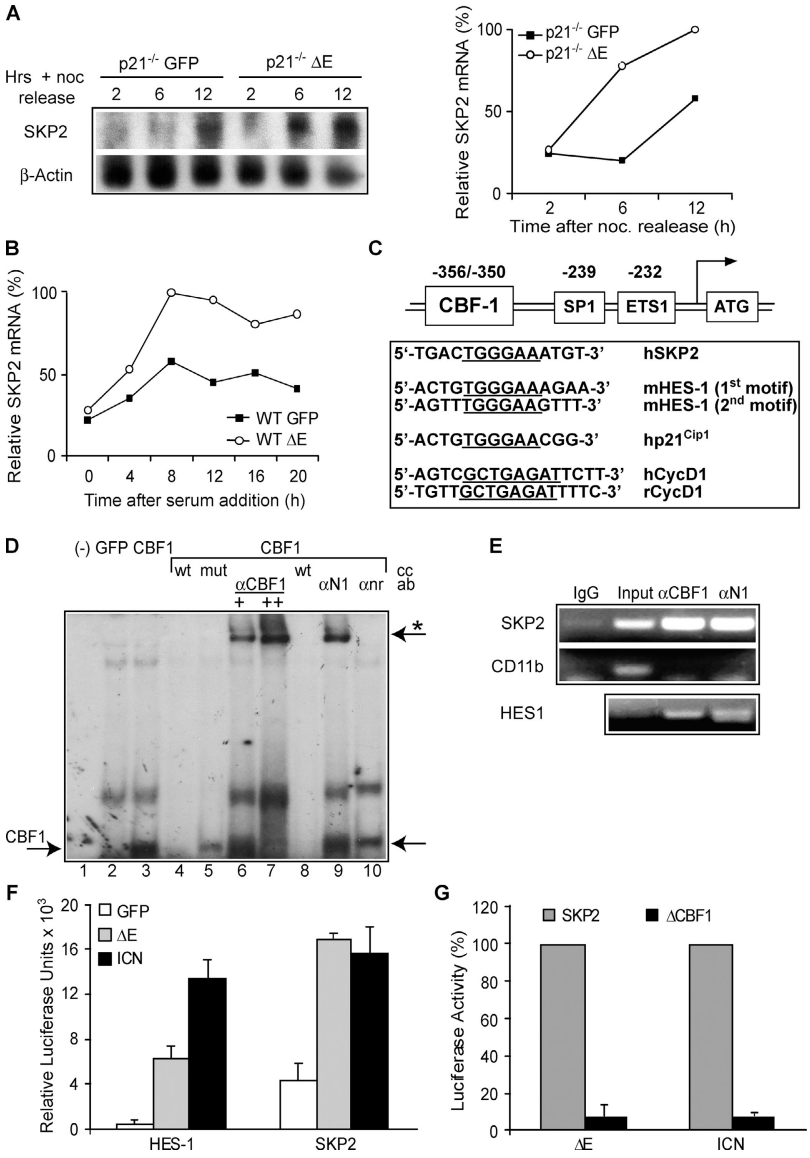

Figure 6. N1 activation induces CBF-1–dependent SKP2 transcription. (A) Kinetics of SKP2 mRNA induction in 3T3 cells synchronized by nocodazole block-release by Northern blot (left panel); the line graph represents percentages of SKP2 expression normalized to β-actin over time (right panel). (B) Transduced 3T3 cells were synchronized by serum starvation and stimulation and were analyzed by Northern blot; values represent percentages of SKP2 expression normalized to β-actin. (C) Identification of CBF-1 binding site in the SKP2 promoter. Top panel: representation of the human SKP2 promoter region containing CBF-1. Bottom panel: comparison of known CBF-1 binding sites in different gene promoters. (D) EMSA analysis was performed by incubating radiolabeled oligonucleotide with no extract (−) or lysates from 293T transfected with GFP or CBF-1. Radiolabeled WT oligonucleotide was incubated with lysates preincubated with 50-fold excess of unlabeled WT (wt) or mutated (mut) oligonucleotide for competition experiments (c.c.), and with unrelated antibody (αnr), anti-N1, or anti-CBF-1 antibodies for supershifts experiments. + and ++ indicate that 2.5 and 5 μl of ab were used. Specific CBF1-DNA complex is indicated as CBF1. (*) indicates the supershifted band obtained when anti–CBF-1 or anti-N1 antibodies were present in the binding mixture. (E) Binding of N1 and CBF1 to the endogenous SKP2 promoter by chromatin IP analysis. SUPT1 cells, which express high levels of activated N1, were processed for chromatin immunoprecipitation with antibodies against CBF-1, N1, or affinity purified IgGs. Input DNA and recovered DNA were analyzed by PCR using specific primers for the indicated promoters. In the Hes1 PCR, the input DNA lane is substituted by a nonimmune IP sample. Positive PCR products were generated from the input DNA. (F) Increased SKP2 and HES-1 promoter activity in the presence of activated N1. Transduced 3T3 cells were transfected with the luciferase reporter plasmid containing the 3.1-kb SKP2 promoter (SKP2-luc) or the HES-1 promoter (HES-luc). Cells were harvested after 40 h and cell extracts were prepared for the luciferase reporter assays. All promoter activity studies are representative of at least three independent experiments. (G) Deletion of CBF-1 binding motif abrogates CBF-1/N1–dependent transcription. Transduced 3T3 cells were transfected with the luciferase reporter plasmid containing the 3.1-kb SKP2 promoter (SKP2-luc) or the site specific deletion in the HES promoter (Δ-CBF1) that abrogate CBF-1/N1–dependent transcription. Cells were harvested after 40 h and cell extracts were prepared for the luciferase reporter assays. Values represent the average percentage of luciferase relative units obtained using the Δ-CBF1 construct relative to SKP2 construct (100%).

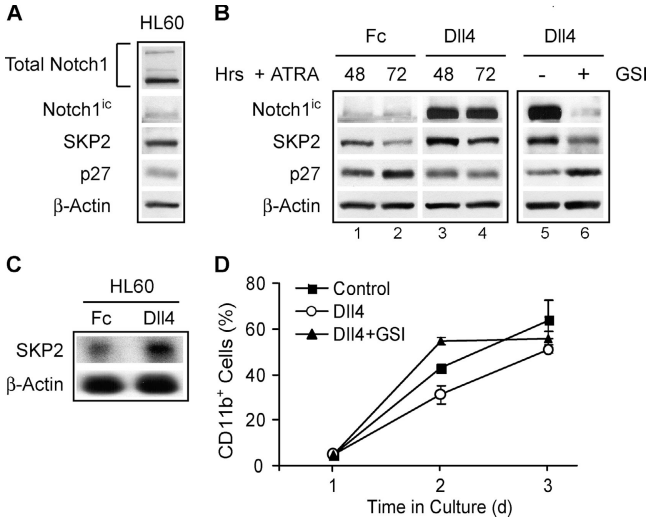

Figure 7. Stimulation of endogenous Notch by Dll4 ligand promotes SKP2 induction in vivo. (A) N1, Notch^{ic}, SKP2, and p27^{Kip1} expression in undifferentiated HL-60 cells. (B) Left panel: HL-60 cells were seeded in wells coated with IgG_1-Fc control fragment (Fc) or recombinant Dll4-Fc fusion protein (Dll4) and cultured in the presence of ATRA. Cell extracts obtained from cells at 48 h and 72 h of culture with Fc or Dll4 and ATRA were analyzed by Western blot using specific antibodies directed to Val 1744-cleaved form of Notch (Notch^{ic}), SKP2, p27^{Kip1}, and β-actin. Right panel: HL-60 cells cultured for 72 h on Fc or Dll4 were incubated with GSI (+) or DMSO vehicle control (−) for an additional 24 h. The white lines indicate that intervening lanes have been spliced out. (C) Northern blot analysis of SKP2 transcripts in HL-60 cells stimulated with Dll4 or Fc fragment for 72 h. (D) HL-60 cells were induced to differentiate in the presence of either ATRA (Co) or ATRA + Dll4 stimulation in the absence or presence of GSI. At the indicated days, cells were analyzed for the expression of the differentiation marker, CD11b, by FACS. Values indicate an average of three independent experiments.

Dll4 stimulation was accompanied by higher levels of SKP2 and failure to accumulate p27^{Kip1} (Fig. 7 B, lanes 3 and 4), whereas in the control, response to ATRA treatment was characterized by SKP2 down-regulation and p27^{Kip1} accumulation (Fig. 7 B, lanes 1 and 2), as documented (26). SKP2 transcripts increased after physiologic stimulation of endogenous N1 by, Dll4 (Fig. 7 C). Dll4 stimulation of Notch signaling was associated with resistance of HL-60 cells to arrest in G_1 and to differentiate (Fig. 7 D)—as we previously reported—with J2 stimulation (6). To prove that SKP2 up-regulation was directly due to Notch activation upon Dll4 stimulation, we treated stimulated HL-60 cells with the Notch inhibitor, GSI. GSI treatment induced a complete inhibition of N1 cleavage, prevented Dll4-mediated induction of SKP2 and which resulted in p27^{Kip1} accumulation (Fig. 7 B, lanes 5 and 6), and promoted cell differentiation (Fig. 7 D). Similarly, expression of a dominant negative form of SKP2 (SKP2ΔF) that prevents p27^{Kip1} degradation (14), increased rates of differentiation in HL-60 cells (Fig. S3, available at http://www.jem.org/cgi/content/full/jem.20050559/DC1) which indicated a direct impact of SKP2 on cell differentiation. These experiments demonstrate that ligand-dependent stimulation of endogenous N1 leads to SKP2 induction and p27^{Kip1} down-regulation, and affects cell differentiation.

Next, we examined whether the loss of N1 had an impact on SKP2 expression and differentiation in vivo. To address this question we used mice transgenic for an N1 antisense (N1AS$^{+/+}$) driven by the mouse mammary tumor virus LTR promoter, which specifically suppresses N1 transcripts in a variety of cell types, including hematopoietic precursors (27, 28). Reduced N1 expression in N1AS$^{+/+}$ correlated with a modest, but reproducible, decrease in SKP2 transcripts (Fig. 8 A) and protein levels (not depicted), when compared with controls (N1AS^{-} and N1AS$^{+/-}$). Analysis of the hematopoietic subsets in N1AS$^{+/+}$ and control mice did not show significant differences in the representation of primitive Lin^{-}Sca^{+} and myeloid mature Gr^{+}/Mac^{+} subsets in the BM and in the spleen (Fig. S4, available at http://www.jem.org/cgi/content/full/jem.20050559/DC1), which is consistent with recent observations made in an inducible knock-out model (29). These data suggest that although N1 activation may have a significant effect on SKP2 induction in adult hematopoietic cells, its absence likely is compensated by other Notch receptors. Evaluation of the Notch/SKP2 pathway should provide more useful information in a model where Notch receptors signaling are abrogated completely.

Finally, we evaluated the effects of Notch stimulation and inhibition in primary hematopoietic cells. BM Lin^{-} cells (enriched in progenitors) were sorted from control mice and were stimulated with Dll4 in the absence or presence of GSI. Dll4 stimulation resulted in induction of SKP2, in a higher fraction of cells in S phase and in a significant higher maintenance of the more primitive subsets Lin^{-}Kit^{+} (Fig. 8, B–D). All of these effects were abolished by the presence of the Notch inhibitor GSI. Taken together, these data show that abrogation of N1 in adult cells results in mild effects, because it is compensated readily by other Notch receptors, whereas an increase in Notch signaling can induce SKP2 and affect cell cycle and differentiation in vivo. Given that Notch ligands can be up-regulated in the BM stroma by hormones, such as parathyroid hormone (30), and by inflammatory cytokines, such as TNF-α (unpublished data), we hypothesize that this mechanism could be of physiologic relevance for hematopoietic progenitors' expansion during BM response to stress conditions.

DISCUSSION

Regulation of the cell cycle, and in particular, of the G_1 checkpoint is one of the fundamental mechanisms underlying determination of cell fate (31). Absence of the critical G_1 regulators CKIs, p21^{Cip1} or p27^{Kip1} or activation of the Notch receptor, a well-known cell fate regulator (1), induce similar alterations in the self-renewal/proliferation/differentiation balance of stem and progenitor cells (4, 5, 11, 12). However, no interaction between these molecular pathways

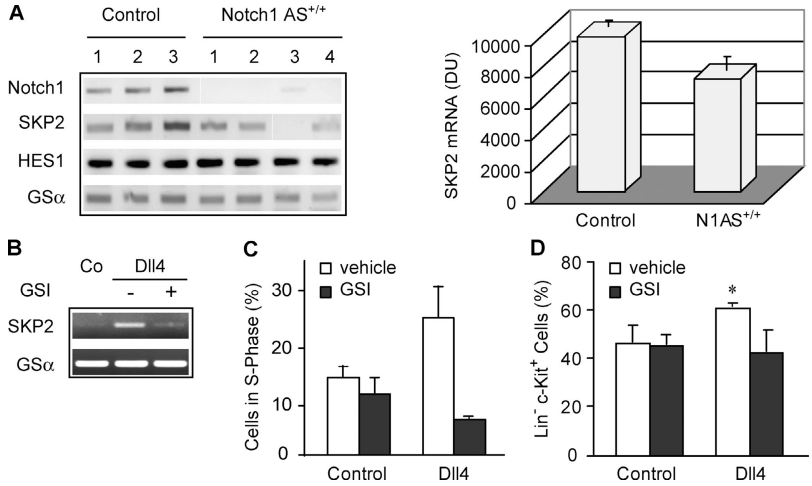

Figure 8. Physiologic relevance of the Notch/SKP2 pathway in vivo. (A) SKP2 expression in the absence of N1. RNA obtained from BM and spleen cells of N1AS$^{+/+}$ and controls were used for RT and PCR amplification for the indicated gene products. All samples were positive for the low molecular size PCR product of the housekeeping gene, GSα, which confirmed the absence of genomic DNA. Noticeable SKP2 expression was found in the spleen cells (left). Bar graph (right) represents densitometric values of SKP2 normalized with GSα (densitometric units, DU); values indicate averages of three controls and four N1AS$^{+/+}$ samples (right; P = 0.064). (B–D) BM Lin$^-$ cells sorted from control mice were exposed to MS5 cells overexpressing vector alone (Co) or Dll4$^{-/+}$ GSI. At day 3, cells were harvested and processed for the following: (B) PCR for SKP2 and GSα and (C) Bromodeoxyuridine incorporation. Bars indicate average percentage of cells in S phase in three independent experiments; difference between control/GSI and Dll4/GSI is not statistically significant. P = 0.1. (D) Immunophenotyping: cells were stained with anti–c-Kit antibody and analyzed by flow cytometer. Bars indicate average percentage of Lin$^-$c-Kit$^+$ cells in three independent experiments. *P = 0.03.

has been defined. The present study provides the first demonstration that the F-box protein, SKP2, links Notch signaling with p27^{Kip1} and p21^{Cip1} regulation.

Rates of G_1-S progression depend on p27^{Kip1} and p21^{Cip1} removal from the CDK2 complexes, either by sequestration by cyclin D-CDK4 complexes or by protein degradation (10). Previous observations correlated Notch activation with lower levels of the CDK inhibitor, p27^{Kip1} (32); however, the direct link to Notch signaling and the mechanism involved have not been investigated. Here, we provide evidence that the Notch signaling pathway regulates the specific degradation of p21^{Cip1} and p27^{Kip1} by directly inducing the transcription of SKP2, the F-box subunit of the ubiquitin-ligase SCF^{SKP2} that targets these CKIs for degradation (14). Notch activation recently was associated with enhanced proteasome-mediated degradation of E47, a molecule involved in lymphoid cell differentiation (33), suggesting that modulation of protein degradation could represent a general mechanism through which Notch signaling modulates cellular processes.

We identified a highly conserved CBF-1 binding motif within the SKP2 promoter region and demonstrated that Notch activation drives SKP2 transcription directly through a CBF-1–dependent mechanism. Notch-mediated SKP2 up-regulation resulted in a more rapid p21^{Cip1} and p27^{Kip1} down-regulation, increased CDK2 activity, and accelerated cell cycle entry. Furthermore, lack of p21^{Cip1} resulted in a more pronounced effect on CDK2 activity and cell cycle progression in the presence of Notch, perhaps by cooperating with decreased levels of p27^{Kip1} in relieving CDK2 inhibition. Depletion of SKP2 by siRNA abrogated Notch-induced p27^{Kip1} down-regulation, and showed that SKP2 is required for Notch-induced p21^{Cip1} and p27^{Kip1} degradation in 3T3 cells. Elimination of the SKP2/CKI pathway reversed the Notch effect on cell cycle entry and resulted in a significant reduction of cells in S phase. However, the effect of Notch on cell cycle entry was not abolished completely in the absence of SKP2; this reinforces the present view that Notch signaling regulates the cell cycle through multiple molecular interactions, as is emerging from several recent reports (34, 35). Although no study has addressed the integrity of the Notch signaling pathway in the SKP2 null cells, SKP2 null mice do not present the obvious abnormalities of the nervous and lymphoid systems derived by altered Notch signaling (20). It is possible that the specific defect in the Notch/SKP2 pathway is compensated by alternative pathways or emerges only under conditions of stress. Similarly, loss of N1 did not result in marked alterations of adult stem and progenitor cells, which suggests a compensatory effect of other Notch receptors.

The physiologic relevance of our findings is confirmed by the demonstration that stimulation of endogenous Notch by its cognate ligand, Dll4, is capable of inducing up-regulation of SKP2 in the hematopoietic cell line HL-60 and in primary progenitor cells. In both models, activation of the Notch/SKP2/CKI pathway correlated with inhibition of progenitor differentiation and with maintenance of more primitive precursors, as described previously (24). It is possible that the Notch/SKP2/CKIs pathway fine tunes the balance of proliferation and differentiation by accelerating entry into cell cycle

and shortening the time spent by cells in G_1, the temporal window where decisions regarding cell cycle withdrawal and differentiation are made. In support of this view, the CKI $p21^{Cip1}$ has been defined as the mediator of the quiescent status of hematopoietic stem cells, as loss of $p21^{Cip1}$ results in a temporary stem cell expansion followed by long-term stem cell exhaustion in vivo (11). Considering that Notch has been shown to induce $p21^{Cip1}$ transcription in some cellular systems (4, 36), and that, in contrast, we observed that it can cause $p21^{Cip1}$ down-regulation, we hypothesized that Notch may regulate hematopoietic stem cell self-renewal through a fine-tuned balance of these two mechanisms. The Notch/SKP2/CKI pathway may have a more defined role in the expansion of hematopoietic progenitors, where $p27^{Kip1}$ plays a critical regulatory function. Notch activation (5, 6, 37) and the loss of $p27^{Kip1}$ (12) promote hematopoietic progenitor expansion. Our studies provide evidence that Notch signaling promotes $p27^{Kip1}$ degradation and suggest that this may be an important regulatory mechanism of hematopoietic progenitors expansion linking microenvironmental cues with the cell cycle effectors.

Neither constitutive loss of p27Kip1 nor constitutive activation of Notch results in myeloid cell transformation or myeloid cell leukemia, suggesting the presence of other negative regulators in the myeloid lineage. In our experimental model, Notch activity alone did not bypass the mitogen requirement for SKP2 induction; this suggests that activation of Notch "per se" is not sufficient to lead to uncontrolled proliferation. Based on these observations, we propose that Notch signaling "primes" SKP2 transcriptional activation during G_1 and S phase entry but needs the presence of conserved cell cycle regulatory mechanisms to accomplish this function successfully. Thus, by anticipating and reinforcing SKP2 induction in the presence of mitogens, Notch signaling accelerates entry into the cell cycle (Fig. 9).

The biologic effects that are induced by Notch signaling are cell context–dependent. In contrast to what is seen in hematopoietic stem and progenitor cells, N1 activation severely compromises T cell development and promotes T cell leukemias (8, 38). In addition, SKP2 was shown to function as an oncoprotein in some cellular contexts (39) and its overexpression is common in leukemias and lymphomas (40). Therefore, it is possible that the capacity of Notch to induce SKP2 and to down-regulate $p27^{Kip1}$ expression may constitute the basis of its oncogenic potential in T lymphoid cells.

In conclusion, we propose that the ability of Notch to modulate a key cell cycle regulator, such as SKP2, plays a role in balancing proliferation/differentiation in the hematopoietic system, and may prove to be critical in cooperating with additional genetic and epigenetic alterations toward the acquisition of a malignant phenotype.

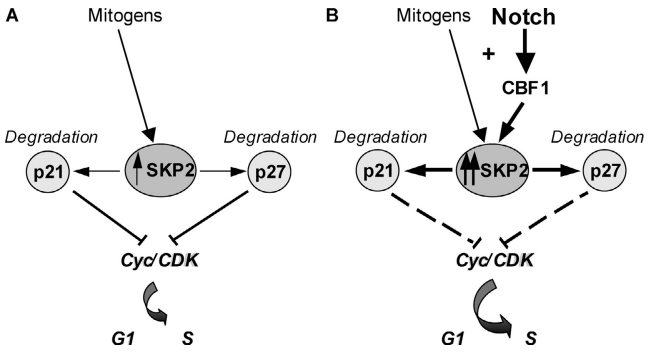

Figure 9. Notch/SKP2/CDK pathway model. (A) In basal conditions, mitogen stimulation promotes reentry into the cell cycle by inducing SKP2 expression, which in turn, mediates $p21^{Cip1}$ and $p27^{Kip1}$ degradation. (B) Activation of Notch by its physiologic ligands synergies with mitogen stimulation and enforces SKP2 transcription, leading to increased degradation of $p21^{Cip1}$ and $p27^{Kip1}$ and to enhanced G_1-S transition.

MATERIALS AND METHODS

cDNA expression constructs and retroviral transduction. N1 ICN and ΔE cDNAs were subcloned into the retroviral vector MSCV-GFP and used for retroviral infections as described (6). GFP-positive cells were sorted by fluorescence-activated cell sorting (FACSVantage; Becton Dickinson). Each individual experiment was performed within 1–2 wk of the transduction and with pools of GFP-expressing cells to avoid the selection bias. Each set of experiments was confirmed by multiple independent transductions.

Cell lines and cell culture. Early passage (20–40) 3T3 fibroblasts were derived from WT and $p21^{-/-}$ mouse embryo as described (16). 293T, 3T3, HL-60, SUP-T1, and MS5 cells were maintained as described (6, 16, 23, 25). Transduced 3T3 cells were treated for 12 h with MG132 (10 μM; Sigma-Aldrich), lactacystin (20 μM; AG Scientific, Fluorochem), vehicle DMSO (1 μl/ml; Sigma-Aldrich); or cycloheximide (Sigma-Aldrich, 50 μg/ml final concentration). 3T3 and HL-60 cells were treated with GSI DFPAA (100 nM; provided by J. Aster, Brigham and Women's Hospital, Boston, MA) or vehicle DMSO (1 μl/ml; Sigma-Aldrich) for 12 h and 24 h. HL-60 cells were seeded at 3×10^5 cells/ml in 6-well plate wells coated with the Fc portion of human IgG (Fc, Jackson ImmunoResearch Laboratories), or with recombinant Dll4 fusion protein consisting of the Dll4 extracellular domain fused to the Fc portion of human IgG (Dll4-Fc) and cultured in RPMI 1640 10% FBS supplemented with 2 μM ATRA (Sigma-Aldrich). Dll4-Fc (10 μg/ml) or Fc (5 μg/ml) was immobilized on culture wells in 1 ml of PBS (Sigma-Aldrich) overnight at 4°C. MS5-vector and MS5-Dll4 cell lines were obtained by transducing MS5 cells with the retroviral vector MSCV-GFP alone or containing the cDNA for Dll4 as described (6).

Mice and primary cultures. C57BL/6 $N1AS^{+/+}$ were generated using a 1164-bp N1AS construct encompassing the 5′ coding region of mouse N1 expressed under the control of the mouse mammary tumor virus LTR promoter as described (27, 28). Hemizygous transgenic mice $N1AS^{+/-}$ were bread to each other, selecting homozygous transgenic $N1AS^{+/+}$ and negative mice. Transgene integration was confirmed by PCR and transgene expression and function were confirmed by RT PCR and Western blot analysis for N1. Age-matched (>16 wk) adult female mice were used. Primary BM cells from C57BL/6 control mice were harvested from femurs and labeled with antibodies directed to lineage markers (Gr1, Mac1, CD3, CD4, CD8, B220, NK, Ter 199). Lin^- (enriched for hematopoietic progenitor cells) were isolated by FACS and seeded on MS5-vector and MS5-Dll4 feeder layers. Lin^- cells were cocultured in IMDM 10% FBS in the absence or presence of 100 nM GSI (Calbiochem); at day 3 of coculture, cells were harvested and processed for evaluation of differentiation, cell cycle, and gene expression.

Cell cycle and cell division analysis. 3T3 cells were synchronized in G_2/M, by treatment with 50 ng/ml of nocodazole (Sigma-Aldrich) for 12 h, and at the G_0/G_1 boundary by serum starvation (0.1% FCS) for 96 h, fol-

lowed by the readdition of serum (10% FCS). The cell cycle was evaluated by bromodeoxyuridine (Sigma-Aldrich) and propidium iodide (Sigma-Aldrich) incorporation followed by analysis with the FACSCalibur flow cytometer and the Cell Quest software (Becton Dickinson). To document cell division history, 3T3 cells labeled with the red fluorescent membrane dye, PKH26-GL (Sigma-Aldrich), were seeded at low density in multiple equivalent wells and each well was harvested every 24 h for 4 d. Collected samples were analyzed by FACS. Cell division profiles were obtained by evaluating the dilution of the dye's mean intensity of fluorescence that occurs at each cell division.

Immunologic reagents and procedures. Immunoprecipitation (IP) and Western blots were performed as described (16). Gel loading was normalized to protein concentration and confirmed by β-actin probing. Signals were quantified using Molecular Dynamics scanner and ImageQuant analysis software. Antibodies used included the intracytoplasmic region of N1 (6); cyclin D1 and CDK4 (for IP, provided by E. Harlow); murine $p21^{Cip1}$ (provided by C. Schneider, Laboratorio Nazionale Biotecnologie, Trieste, Italy); CBF-1/RBP-Jκ (provided by E. Kieff, Brigham and Women's Hospital, Boston, MA; reference 41; Fig. S5, available at http://www.jem.org/cgi/content/full/jem.20050559/DC1); $p27^{Kip1}$ (K25020; Transduction Laboratories); and $Notch^{ic}$ (Val 1744; 2421, Cell Signal); and the following: cyclin A (H-432), cyclin E (M-20), CDK2 (M2), CDK4 (C-22), SKP2 (H-435), and β-actin (I-19), obtained from Santa Cruz Biotechnology, Inc. Detection of in vivo $p27^{Kip1}$-ubiquitin conjugates was performed as described (21). Lysates (1.5 mg total protein) were IP with anti-$p27^{Kip1}$ antibody (C-19, Santa Cruz Biotechnology, Inc.) and $p27^{Kip1}$ forms were detected by immunoblotting (K25020; Transduction Laboratories).

Silencing by small interfering RNA. 3T3 cells seeded at a 30–40% density were serum starved for 96 h before serum (10% FCS) readdition. The siRNA duplexes that were used for silencing SKP2 or GFP (negative control) were 21-bp synthetic oligonucleotides synthesized by Dharmacon Research (SMARTpool). Two rounds of transfections were carried on for 12 h using lipofectamine 2000 reagent (Invitrogen) as recommended.

SKP2 promoter cloning and luciferase assays. The human SKP2 promoter region was identified by analysis of the human genome database and analyzed for regulatory motifs using the Genome Exploring and Modelling Software (GEMS) by Genomatix. A region from −3136 to +154, including the first exon (GenBank sequence accession no. U 33761), was amplified by PCR using genomic DNA of HL-60 cells and cloned into the pGEM-T easy vector (Promega). A 3074-bp fragment was subcloned in the SmaI site of the pGL2-basic vector (Promega) containing the luciferase gene. The primers used for cloning are: forward 5′-TACAATGAATTAAAGATCTACTTAGTTCCAAGC-3′ (−3136 to −3103); reverse 5′-ATTCACTTAACAGCATTACTAACAATATTAGCC-3′ (+121 to +154).

HES-1luc and ΔCBF-1-luc luciferase assays were performed using the HES-1AB and HES-1ΔAB pGL2 constructs (42). For each experiment, triplicate wells of 3T3 cells were transfected transiently with pGL2, SKP2-pGL2, ΔCBF-1-pGL2, or HES-1-pGL2 together with pSV-β-galactosidase (Promega). Cells were harvested 36–40 h after transfection; luciferase activity was measured in each sample using a Luciferase Assay kit (Promega) and TR 717 microplate luminometer (Applied Biosystems). Luciferase readings were normalized for β-galactosidase activity for each sample.

Northern blot analysis, electrophoretic mobility shift assay, chromatin immunoprecipitation, and PCR. RNAs were extracted using Tri-Reagent (Sigma-Aldrich). Double-strand DNA probes were labeled using the Prime-it II Random primer labeling kit (Stratagene) and α ^{32}P-dATP (Amersham Biosciences). Probes: the 700-bp 5′ BamHI fragment from human SKP2 cDNA (provided by B. Schulman, St. Jude Children's Research Hospital, Memphis, TN) and the 429-bp fragment (+703 to +1131) of mouse β-actin.

For EMSA analysis, 293T cells were transfected transiently with pcDNA-GFP or CBF-1 and lysed in the 5× extraction buffer. Binding reactions were carried on using the γ-^{32}P–end-labeled double-stranded oligonucleotide probe containing the CBF-1 binding site. For supershift experiments, 5 μl of rabbit polyclonal anti–CBF-1/RBP-Jκ, anti-N1, an unrelated rabbit antibody (directed to the G-protein SGPR1) or rabbit IgGs, were incubated with the cell extracts before addition of the labeled oligonucleotide. The oligonucleotides sequences containing the CBF-1 binding motif and surrounding regions of the SKP2 promoter were: 5′-CGCTACGGCTGAC*TGGGAA*ATGTCAGCCGCTGGA-3′ (WT) and 5′-CGCTACGGCTGAC*CT*GGAAATGTCAGCCGCTGGA-3′ (mutant).

Chromatin preparation from SUP-T1 cells was cross-linked with endogenous DNA and immunoprecipitated with anti–CBF-1 or anti-N1 antibodies as described (43). Recovered DNA was analyzed by PCR amplification. Preliminary experiments with necked DNA were performed to optimize PCR conditions. The following primers were used to amplified promoter regions for: SKP2 (200 bp) F: 5′-GATCCACGCTCAGAGACGAC-3′, R: 5′-CCTTCCCTTGCAGCTTTACC-3′; Hes1 (120 bp) F: 5′-CCAAAGACAGCATCTGAGCAC-3′, R: 5′-GAACGCAGTACCAGCGAGTG-3′; and CD11b (100 bp) F: 5′-GACCAGGCAGGGCTATGT-3′, R: 5′-AAAGCAAAGAAGGGCAGAAA-3′.

RNA from BM, spleen, and sorted Lin^- cells was extracted using Trizol (Invitrogen). RNA treated with DNase (Ambion) was used for RT reaction and PCR. The primers used were: N1: F: 5′-CGGTGTGAGGGTGATGTCAATG-3′, R: 5′-GAATGTCCGGGCCAGCGCCACC-3′; SKp2: F: 5′-GAGCCAACTCTTCCAAGTGC-3′, R: 5′-AATCCTGCACCAATCCTGTC-3′; Hes1: F: 5′-AACACGACACCGGACAAAC-3′, R: 5′-GAATGCCGGGAGCTATCTT-3′. The primers for the housekeeping gene GSα (44), F: 5′-GCTGCTGGCCACCACGAAGAT-3′, R: 5′-GTGATCAAGCAGGCTGACTAT-3′, allow discrimination of contaminating genomic DNA by identification of a high molecular product containing an intervening intron. PCR conditions: 95 5′; (95 1′; 64 1′; 72 1.5′) × 32 cycles; 72 10′.

Statistical analysis. Equality of distributions for matched pairs of observations was tested using the *t* test.

Online supplemental materials. Fig. S1 shows retroviral transduction. Fig. S2 shows effects of proteasome inhibition by MG132. Figs. S3 shows effect of SKP2 inhibition on cell differentiation. Fig. S4 shows hematopoietic subsets in the absence of Notch1. Fig. S5 shows specificity of the antibody directed to CBF1/RBP-Jκ. Online supplemental material is available at http://www.jem.org/cgi/content/full/jem.20050559/DC1.

We thank D.T. Scadden, P. Christmas, R. Soberman, and J. Settleman for critical comments, and F. Cristina and L. Fernandez for technical assistance. This work was supported by NIH R01 HL68256-01 (to N. Carlesso), the Foundation for Science and Technology (FCT-Portugal), DAMD17-02-C0125 (to A. Limon), Claflin Award (to N. Carlesso and M. Classon). L.M. Sarmento and M.J. Tavares were funded by a scholarship from FCT-Portugal.

The authors have no conflicting financial interests.

Submitted: 15 March 2005
Accepted: 19 May 2005

REFERENCES

1. Artavanis-Tsakonas, S., M.D. Rand, and R.J. Lake. 1999. Notch signaling: cell fate control and signal integration in development. *Science*. 284:770–776.
2. De Strooper, B., W. Annaert, P. Cupers, P. Saftig, K. Craessaerts, J.S. Mumm, E.H. Schroeter, V. Schrijvers, M.S. Wolfe, W.J. Ray, et al. 1999. A presenilin-1-dependent gamma-secretase-like protease mediates release of Notch intracellular domain. *Nature*. 398:518–522.
3. Davis, R.L., and D.L. Turner. 2001. Vertebrate hairy and Enhancer of split related proteins: transcriptional repressors regulating cellular differentiation and embryonic patterning. *Oncogene*. 20:8342–8357.
4. Rangarajan, A., C. Talora, R. Okuyama, M. Nicolas, C. Mammucari, H. Oh, J.C. Aster, S. Krishna, D. Metzger, P. Chambon, et al. 2001. Notch signaling is a direct determinant of keratinocyte growth arrest

and entry into differentiation. *EMBO J.* 20:3427–3436.
5. Stier, S., T. Cheng, D. Dombkowski, N. Carlesso, and D.T. Scadden. 2002. Notch1 activation increases hematopoietic stem cell self-renewal in vivo and favors lymphoid over myeloid lineage outcome. *Blood.* 99: 2369–2378.
6. Carlesso, N., J.C. Aster, J. Sklar, and D.T. Scadden. 1999. Notch1-induced delay of human hematopoietic progenitor cell differentiation is associated with altered cell cycle kinetics. *Blood.* 93:838–848.
7. Ronchini, C., and A.J. Capobianco. 2001. Induction of cyclin D1 transcription and CDK2 activity by Notch(ic): implication for cell cycle disruption in transformation by Notch(ic). *Mol. Cell. Biol.* 21:5925–5934.
8. Pear, W.S., J.C. Aster, M.L. Scott, R.P. Hasserjian, B. Soffer, J. Sklar, and D. Baltimore. 1996. Exclusive development of T cell neoplasms in mice transplanted with bone marrow expressing activated Notch alleles. *J. Exp. Med.* 183:2283–2291.
9. Nicolas, M., A. Wolfer, K. Raj, J.A. Kummer, P. Mill, M. Van Noort, C.C. Hui, H. Clevers, G.P. Dotto, and F. Radtke. 2003. Notch1 functions as a tumor suppressor in mouse skin. *Nat. Genet.* 33:416–421.
10. Sherr, C.J., and J.M. Roberts. 1999. CDK inhibitors: positive and negative regulators of G1-phase progression. *Genes Dev.* 13:1501–1512.
11. Cheng, T., N. Rodrigues, H. Shen, Y. Yang, D. Dombkowski, M. Sykes, and D.T. Scadden. 2000. Hematopoietic stem cell quiescence maintained by p21cip1/waf1. *Science.* 287:1804–1808.
12. Cheng, T., N. Rodrigues, D. Dombkowski, S. Stier, and D.T. Scadden. 2000. Stem cell repopulation efficiency but not pool size is governed by p27(kip1). *Nat. Med.* 6:1235–1240.
13. Fero, M.L., M. Rivkin, M. Tasch, P. Porter, C.E. Carow, E. Firpo, K. Polyak, L.H. Tsai, V. Broudy, R.M. Perlmutter, et al. 1996. A syndrome of multiorgan hyperplasia with features of gigantism, tumorigenesis, and female sterility in p27(Kip1)-deficient mice. *Cell.* 85:733–744.
14. Carrano, A.C., E. Eytan, A. Hershko, and M. Pagano. 1999. SKP2 is required for ubiquitin-mediated degradation of the CDK inhibitor p27. *Nat. Cell Biol.* 1:193–199.
15. Bornstein, G., J. Bloom, D. Sitry-Shevah, K. Nakayama, M. Pagano, and A. Hershko. 2003. Role of the SCFSkp2 ubiquitin ligase in the degradation of p21Cip1 in S phase. *J. Biol. Chem.* 278:25752–25757.
16. Classon, M., S. Salama, C. Gorka, R. Mulloy, P. Braun, and E. Harlow. 2000. Combinatorial roles for pRB, p107, and p130 in E2F-mediated cell cycle control. *Proc. Natl. Acad. Sci. USA.* 97:10820–10825.
17. Berezovska, O., C. Jack, P. McLean, J.C. Aster, C. Hicks, W. Xia, M.S. Wolfe, W.T. Kimberly, G. Weinmaster, D.J. Selkoe, and B.T. Hyman. 2000. Aspartate mutations in presenilin and gamma-secretase inhibitors both impair notch1 proteolysis and nuclear translocation with relative preservation of notch1 signaling. *J. Neurochem.* 75:583–593.
18. Weng, A.P., Y. Nam, M.S. Wolfe, W.S. Pear, J.D. Griffin, S.C. Blacklow, and J.C. Aster. 2003. Growth suppression of pre-T acute lymphoblastic leukemia cells by inhibition of notch signaling. *Mol. Cell. Biol.* 23:655–664.
19. Pagano, M., S.W. Tam, A.M. Theodoras, P. Beer-Romero, G. Del Sal, V. Chau, P.R. Yew, G.F. Draetta, and M. Rolfe. 1995. Role of the ubiquitin-proteasome pathway in regulating abundance of the cyclin-dependent kinase inhibitor p27. *Science.* 269:682–685.
20. Nakayama, K., H. Nagahama, Y.A. Minamishima, M. Matsumoto, I. Nakamichi, K. Kitagawa, M. Shirane, R. Tsunematsu, T. Tsukiyama, N. Ishida, et al. 2000. Targeted disruption of Skp2 results in accumulation of cyclin E and p27(Kip1), polyploidy and centrosome overduplication. *EMBO J.* 19:2069–2081.
21. Spruck, C., H. Strohmaier, M. Watson, A.P. Smith, A. Ryan, T.W. Krek, and S.I. Reed. 2001. A CDK-independent function of mammalian Cks1: targeting of SCF(Skp2) to the CDK inhibitor p27Kip1. *Mol. Cell.* 7:639–650.
22. Tun, T., Y. Hamaguchi, N. Matsunami, T. Furukawa, T. Honjo, and M. Kawaichi. 1994. Recognition sequence of a highly conserved DNA binding protein RBP-J kappa. *Nucleic Acids Res.* 22:965–971.
23. Aster, J.C., E.S. Robertson, R.P. Hasserjian, J.R. Turner, E. Kieff, and J. Sklar. 1997. Oncogenic forms of NOTCH1 lacking either the primary binding site for RBP-Jkappa or nuclear localization sequences retain the ability to associate with RBP-Jkappa and activate transcription. *J. Biol. Chem.* 272:11336–11343.
24. Milner, L.A., and A. Bigas. 1999. Notch as a mediator of cell fate determination in hematopoiesis: evidence and speculation. *Blood.* 93: 2431–2448.
25. Bennaceur-Griscelli, A., C. Tourino, B. Izac, W. Vainchenker, and L. Coulombel. 1999. Murine stromal cells counteract the loss of long-term culture-initiating cell potential induced by cytokines in CD34(+) CD38(low/neg) human bone marrow cells. *Blood.* 94:529–538.
26. Dow, R., J. Hendley, A. Pirkmaier, E.A. Musgrove, and D. Germain. 2001. Retinoic acid-mediated growth arrest requires ubiquitylation and degradation of the F-box protein Skp2. *J. Biol. Chem.* 276:45945–45951.
27. Yasutomo, K., C. Doyle, L. Miele, C. Fuchs, and R.N. Germain. 2000. The duration of antigen receptor signalling determines CD4+ versus CD8+ T-cell lineage fate. *Nature.* 404:506–510.
28. Cheng, P., A. Zlobin, V. Volgina, S. Gottipati, B. Osborne, E.J. Simel, L. Miele, and D.I. Gabrilovich. 2001. Notch-1 regulates NF-kappaB activity in hemopoietic progenitor cells. *J. Immunol.* 167:4458–4467.
29. Mancini, S.J., N. Mantei, A. Dumortier, U. Suter, H.R. Macdonald, and F. Radtke. 2004. Jagged1 dependent Notch signaling is dispensable for hematopoietic stem cell self-renewal and differentiation. *Blood.* 105: 2340–2342.
30. Calvi, L.M., G.B. Adams, K.W. Weibrecht, J.M. Weber, D.P. Olson, M.C. Knight, R.P. Martin, E. Schipani, P. Divieti, F.R. Bringhurst, et al. 2003. Osteoblastic cells regulate the haematopoietic stem cell niche. *Nature.* 425:841–846.
31. Pardee, A.B. 1989. G1 events and regulation of cell proliferation. *Science.* 246:603–608.
32. Cereseto, A., and S. Tsai. 2000. Jagged2 induces cell cycling in confluent fibroblasts susceptible to density-dependent inhibition of cell division. *J. Cell. Physiol.* 185:425–431.
33. Nie, L., M. Xu, A. Vladimirova, and X.H. Sun. 2003. Notch-induced E2A ubiquitination and degradation are controlled by MAP kinase activities. *EMBO J.* 22:5780–5792.
34. Rao, P., and T. Kadesch. 2003. The intracellular form of notch blocks transforming growth factor beta-mediated growth arrest in Mv1Lu epithelial cells. *Mol. Cell. Biol.* 23:6694–6701.
35. Bocchetta, M., L. Miele, H.I. Pass, and M. Carbone. 2003. Notch-1 induction, a novel activity of SV40 required for growth of SV40-transformed human mesothelial cells. *Oncogene.* 22:81–89.
36. Sriuranpong, V., M.W. Borges, R.K. Ravi, D.R. Arnold, B.D. Nelkin, S.B. Baylin, and D.W. Ball. 2001. Notch signaling induces cell cycle arrest in small cell lung cancer cells. *Cancer Res.* 61:3200–3205.
37. Varnum-Finney, B., C. Brashem-Stein, and I.D. Bernstein. 2003. Combined effects of Notch signaling and cytokines induce a multiple log increase in precursors with lymphoid and myeloid reconstituting ability. *Blood.* 101:1784–1789.
38. Ellisen, L.W., J. Bird, D.C. West, A.L. Soreng, T.C. Reynolds, S.D. Smith, and J. Sklar. 1991. TAN-1, the human homolog of the Drosophila notch gene, is broken by chromosomal translocations in T lymphoblastic neoplasms. *Cell.* 66:649–661.
39. Pagano, M., and R. Benmaamar. 2003. When protein destruction runs amok, malignancy is on the loose. *Cancer Cell.* 4:251–256.
40. Latres, E., R. Chiarle, B.A. Schulman, N.P. Pavletich, A. Pellicer, G. Inghirami, and M. Pagano. 2001. Role of the F-box protein Skp2 in lymphomagenesis. *Proc. Natl. Acad. Sci. USA.* 98:2515–2520.
41. Robertson, E.S., S. Grossman, E. Johannsen, C. Miller, J. Lin, B. Tomkinson, and E. Kieff. 1995. Epstein-Barr virus nuclear protein 3C modulates transcription through interaction with the sequence-specific DNA-binding protein J kappa. *J. Virol.* 69:3108–3116.
42. Jarriault, S., C. Brou, F. Logeat, E.H. Schroeter, R. Kopan, and A. Israel. 1995. Signalling downstream of activated mammalian Notch. *Nature.* 377:355–358.
43. Orlando, V., H. Strutt, and R. Paro. 1997. Analysis of chromatin structure by in vivo formaldehyde cross-linking. *Methods.* 11:205–214.
44. Nikolic, B., J.P. Gardner, D.T. Scadden, J.S. Arn, D.H. Sachs, and M. Sykes. 1999. Normal development in porcine thymus grafts and specific tolerance of human T cells to porcine donor MHC. *J. Immunol.* 162:3402–3407.